A NONLINEAR ELECTROMECHANICAL PENDULUM ARM WITH A NONLINEAR ENERGY SINK CONTROL (NES) APPROACH

G. Füsun Alişverişçi, Hüseyin Bayiroğlu

Yıldız Technical University, Istanbul, Turkey; e-mail: afusun@yildiz.edu.tr; hbayir@yildiz.edu.tr

Jorge Luis Palacios Felix

UFFS – Federal University of Fronteira Sul, Cerro Largo, RS, Brazil; e-mail: jorge.felix@uffs.edu.br

José M. Balthazar

ITA – Aeronautics Technological Institute, São José dos Campos, SP, Brazil and UNESP-Bauru, SP, Brazil
e-mail: jmbaltha@gmail.com

Reyolando Manoel Lopes Rebello da Fonseca Brasil

Federal University of ABC, Santo André, SP, Brazil; e-mail: reyolando.brasil@ufabc.edu.br

This paper considers the nonlinear dynamics of an electromechanical device with a pendulum arm and a Nonlinear Energy Sink (NES) put on the point of the pendulum suspension. It is shown that the (NES) is capable of absorbing energy from the system. The numerical results are shown in a bifurcation diagram, phase plane, Poincaré map and Lyapunov exponents.

Keywords: nonlinear electromechanical system, bifurcations, nonlinear energy sink

1. Introduction

Mechanical oscillatory systems (e.g., a pendulum system which is a basic subsystem of any robot) are of special interest for research and applications as examples of simple systems that may exhibit complex nonlinear behavior. That is why mechanical pendulum-like models of robot arms and mechanical manipulators have recently drawn attention of researchers (Mogo and Woafo, 2007). An interesting example of a driven pendulum device coupled with an electric circuit through a magnetic field. This enters the class of nonlinear electromechanical devices with a pendulum arm. It has been found that the device displays different nonlinear behavior, including chaos (Mogo and Woafo, 2007). SDRE control and sensibility analysis of a chaotic double pendulum arm excited by a RLC circuit based nonlinear shaker was presented by Tusset *et al.* (2014, 2015). A non-ideal electromechanical damping vibration absorber, the Sommerfeld effect and energy transfer were studied by Felix and Balthazar (2009). The energy pumping, synchronization and beat phenomenon in a non-ideal structure coupled with an essentially nonlinear oscillator were discussed by Felix *et al.* (2009).

This paper deals with a thin rod mounted to a plate to which electrical windings are applied. Connected to an electric circuit (Tusset *et al.*, 2014, 2015), its oscillations are due to the electromagnetic force resulting from two identical and repulsive permanent magnets (Mogo and Woafo, 2007) as well as a Nonlinear Energy Sink. NES has recently drawn attention of many researchers. The NES method represents a new and unique application of strong nonlinearity. The nonlinear energy sink is a local, simple, lightweight subsystem capable of completely altering the global behavior of the primary system to which it is attached (Vakakis *et al.*, 2008). Elimination of chaotic behavior in a non-ideal portal frame structural system using both passive and active controls were described by Tusset *et al.* (2013). Steady-state dynamics of a linear

structure weakly coupled to an essentially nonlinear oscillator was studied by Malatkar and Nayfeh (2007).

Steady state passive nonlinear energy pumping in coupled oscillators was studied by Jiang *et al.* (2003). Introduction of passive nonlinear energy sinks to linear systems was discussed by Vakakis (2001). Energy pumping in nonlinear mechanical oscillators for resonance capture was examined by Vakakis and Gendelman (2001). The energy transfer between linear and non-linear oscillators was investigated by Dantas and Balthazar (2008).
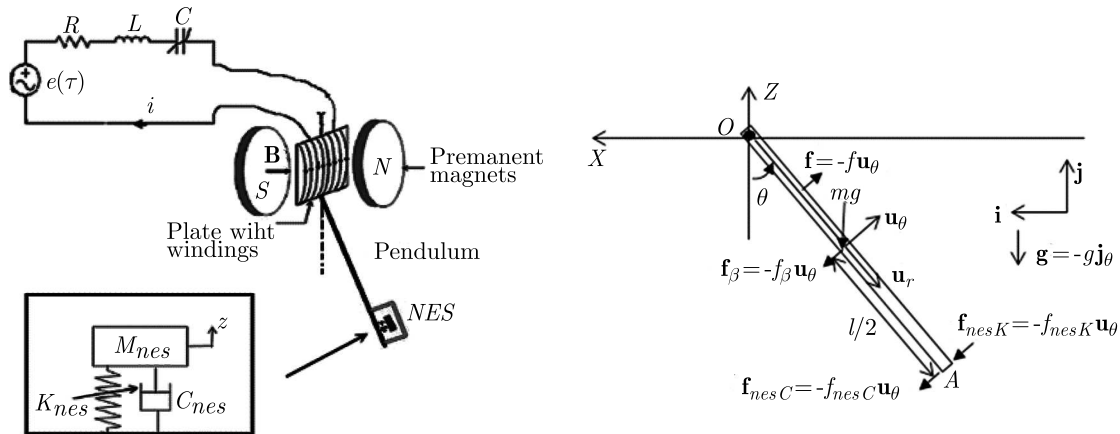

Fig. 1. Idealization of a NES applied to a pendulum arm, $\mathbf{u}_r$ and $\mathbf{u}_\theta$ are the polar unit vectors

In this work, a NES device is applied to the free end of the pendulum (Fig. 1). This set-up is a system with three degrees of freedom: (i) charge q of the nonlinear condenser, (ii) angular displacement θ of the pendulum, (iii) displacement ζ of the M_{nes}.

2. Equations of motion

2.1. Equation of the electric drive

The electric oscillator used to drive the pendulum is an RLC series circuit with a sinusoidal excitation $e(t) = v_0 \cos \Omega t$ (v_0 and Ω being, respectively, the amplitude and frequency, and t time). Denoting the forced mesh current i in the RLC circuit, as shown in Fig. 1, applying Kirchhoff's rules, and taking into account the contribution of Lenz's electromotive voltage for N turns by integrating over θ from zero to $2\pi N$ ($e = -0.5NB\sigma^2 l^2 \, d\theta/dt$) one obtains

$$L\frac{di}{dt} + Ri + V_c(q) - e = e(t) \tag{2.1}$$

where $L\,di/dt$, Ri, $V_C(q)$ are the voltages across the selenoid of the inductance L, the resistor R, and the nonlinear capacitor C, respectively. In this electromechanical model, the electrical nonlinear term is introduced by considering that the voltage of the capacitor is a nonlinear function of the instantaneous electrical charge q of the following form

$$V_c(q) = \frac{1}{C_0}q + a_3 q^3 \tag{2.2}$$

where C_0 is the linear value of C and a_3 is the nonlinear coefficient depending on the type of the capacitor used. Inserting Eq. (2.2) in Eq. (2.1), the electric part of the model is described by the following nonlinear differential equation

$$\frac{d^2q}{dt^2} + \frac{R}{L}\frac{dq}{dt} + \omega_e^2 q + \frac{a_3}{L}q^3 + \frac{NB\sigma^2 l^2}{2L}\frac{d\theta}{dt} = \frac{v_0}{L}\cos(\Omega t) \tag{2.3}$$

where $\omega_e^2 = 1/(LC_0)$ is the resonance frequency of the electric oscillator.

2.2. Equation of the pendulum arm and the Nonlinear Energy Sink

In Fig. 1, the forces acting on the pendulum are represented. The mechanism consists of a uniform thin rod OA of mass m and length l, having a plate to which N conducting electric windings of length σl each are applied, with $\sigma = 1/2$. The pendulum is hinged at O about a horizontal axis, with only the portion σl of the rod in the magnetic field. The total mass of the conducting wire and the plate bathing in the magnetic field have been neglected compared to the pendulum mass. The moment of inertia of the output is then reduced to

$$I_O = \frac{1}{3}ml^2 + M_{nes}l^2 \tag{2.4}$$

where m, M_{nes} are mass of the pendulum and NES, respectively. When the current i flows through the conducting wire in the magnetic field, there appear, according to the directions of the current (upward or downward), two identical Laplace forces (direction and intensity) whose resultant f sets the pendulum into motion in a viscous medium with the frictional coefficient β. According to the equation for kinetic moment, the moment of inertia I_O times the angular acceleration equals the sum of torques due to forces applied to the pendulum. The Laplace force $f = NB\sigma l\, dq/dt$ is applied to the center of the plate gravity and friction forces. NES spring and friction forces are applied to the free end of the pendulum.

Thus, the pendulum motion is described by

$$I_O \frac{d^2\theta}{dt^2} = \frac{NB\sigma^2 l^2}{2}\frac{dq}{dt} - \frac{mgl}{2}\sin\theta - \frac{\beta l^2}{4}\frac{d\theta}{dt} - C_{nes}l\Big(l\frac{d\theta}{dt} - \frac{d\zeta}{dt}\Big) - K_{nes}l(l\theta - \zeta)^n \tag{2.5}$$

where $n = 1$ and $n = 3$. It can be divided by the moment of inertia to obtain this equation in the standard form

$$\begin{aligned}
\frac{d^2\theta}{dt^2} &= \frac{NB\sigma^2 l^2}{2\big(\frac{m}{3}+M_{nes}\big)l^2}\frac{dq}{dt} - \frac{mgl}{2\big(\frac{m}{3}+M_{nes}\big)l^2}\sin\theta - \frac{\beta l^2}{4\big(\frac{m}{3}+M_{nes}\big)l^2}\frac{d\theta}{dt} \\
&\quad - \frac{C_{nes}l}{\big(\frac{m}{3}+M_{nes}\big)l^2}\Big(l\frac{d\theta}{dt} - \frac{d\zeta}{dt}\Big) - \frac{K_{nes}l}{\big(\frac{m}{3}+M_{nes}\big)l^2}(l\theta - \zeta)^n \\
\frac{d^2\theta}{dt^2} &+ \omega_m^2\sin\theta + \frac{\beta}{4\big(\frac{m}{3}+M_{nes}\big)}\frac{d\theta}{dt} - \frac{NB\sigma^2}{2\big(\frac{m}{3}+M_{nes}\big)}\frac{dq}{dt} + \frac{C_{nes}}{\big(\frac{m}{3}+M_{nes}\big)l}\Big(l\frac{d\theta}{dt} - \frac{d\zeta}{dt}\Big) \\
&+ \frac{K_{nes}}{\big(\frac{m}{3}+M_{nes}\big)l}(l\theta - \zeta)^n = 0
\end{aligned} \tag{2.6}$$

where $\omega_m^2 = mg/[2(\frac{m}{3}+M_{nes})l]$ is the resonance frequency of the pendulum, C_{nes} is the damping coefficients of the NES, K_{nes} is the spring coefficient of the NES.

According to Newton's second law, the NES motion is described by

$$M_{nes}\frac{d^2\zeta}{dt^2} = -C_{nes}\Big(\frac{d\zeta}{dt} - l\frac{d\theta}{dt}\Big) - K_{nes}(\zeta - l\theta)^n \tag{2.7}$$

It can be divided by mass of the NES to obtain this equation in the standard form

$$\frac{d^2\zeta}{dt^2} + \frac{C_{nes}}{M_{nes}}\Big(\frac{d\zeta}{dt} - l\frac{d\theta}{dt}\Big) + \frac{K_{nes}}{M_{nes}}(\zeta - l\theta)^n = 0 \tag{2.8}$$

2.3. Nondimensional equations and values of the parameter

Using the transformation

$$x = \frac{q}{Q_0} \qquad\qquad y = \frac{\theta}{\theta_0} \qquad\qquad z = \frac{\zeta}{l\theta_0} \qquad\qquad \tau = \omega_e t$$

$$\frac{dq}{dt} = Q_0\omega_e\frac{dx}{d\tau} \qquad \frac{d\theta}{dt} = \theta_0\omega_e\frac{dy}{d\tau} \qquad \frac{d\zeta}{dt} = l\theta_0\omega_e\frac{dz}{d\tau} \qquad\qquad (2.9)$$

$$\frac{d^2q}{dt^2} = Q_0\omega_e^2\frac{d^2x}{d\tau^2} \qquad \frac{d^2\theta}{dt^2} = \theta_0\omega_e^2\frac{d^2y}{d\tau^2} \qquad \frac{d^2\zeta}{dt^2} = l\theta_0\omega_e^2\frac{d^2z}{d\tau^2}$$

where x, y, τ are dimensionless variables, Q_0 is the reference charge of the condenser, and θ_0 is the reference pendulum angular displacement. The equations of motion of the complete system can be written as follows

$$\frac{d^2x}{d\tau^2} + \frac{R}{L\omega_e}\frac{dx}{d\tau} + x + \frac{a_3Q_0^2}{L\omega_e^2}x^3 + \frac{NB\sigma^2l^2\theta_0}{2LQ_0\omega_e}\frac{dy}{d\tau} = \frac{v_0}{Q_0\omega_e^2L}\cos\left(\frac{\Omega}{\omega_e}\tau\right)$$

$$\frac{d^2y}{d\tau^2} = \frac{NB\sigma^2}{2\left(\frac{m}{3}+M_{nes}\right)\omega_e\theta_0}Q_0\frac{dx}{d\tau} - \frac{mg}{2\left(\frac{m}{3}+M_{nes}\right)\theta_0\omega_e^2l}\sin(\theta_0y) - \frac{\beta}{4\left(\frac{m}{3}+M_{nes}\right)\omega_e}\frac{dy}{d\tau}$$

$$\qquad - \frac{C_{nes}}{\left(\frac{m}{3}+M_{nes}\right)\omega_e}\left(\frac{dy}{d\tau}-\frac{dz}{d\tau}\right) - \frac{K_{nes}(l\theta_0)^{n-1}}{\left(\frac{m}{3}+M_{nes}\right)\omega_e^2}(y-z)^n \qquad\qquad (2.10)$$

$$\frac{d^2z}{d\tau^2} + \frac{C_{nes}}{M_{nes}\omega_e}\left(\frac{dz}{d\tau}-\frac{dy}{d\tau}\right) + \frac{K_{nes}(l\theta_0)^{n-1}}{M_{nes}\omega_e^2}(z-y)^n = 0$$

and

$$x'' + \mu_1x' + x + \alpha x^3 + \gamma_1 y' = E\cos(\omega\tau)$$
$$y'' + \mu_2 y' + \omega_2^2\sin(\theta_0'y) - \gamma_2 x' + c_{2nes}(y'-z') + k_{2nes}(y-z)^n = 0 \qquad\qquad (2.11)$$
$$z'' + c_{1nes}(z'-y') + k_{1nes}(z-y)^n = 0$$

where the prime denotes a derivative with respect to τ and

$$\mu_1 = \frac{R}{L\omega_e} \qquad\qquad \alpha = \frac{a_3Q_0^2}{L\omega_e^2} \qquad\qquad E = \frac{v_0}{LQ_0\omega_e^2}$$

$$\omega = \frac{\Omega}{\omega_e} \qquad\qquad \gamma_1 = \frac{NB\sigma^2l^2\theta_0}{2LQ_0\omega_e} \qquad\qquad \mu_2 = \frac{\beta}{4\left(\frac{m}{3}+m_{nes}\right)\omega_e}$$

$$\omega_2^2 = \frac{\omega_m^2}{\omega_e^2\theta_0} \qquad\qquad \gamma_2 = \frac{NB\sigma^2Q_0}{2\left(\frac{m}{3}+m_{nes}\right)\omega_e\theta_0} \qquad\qquad c_{1nes} = \frac{C_{nes}}{m_{nes}\omega_e}$$

$$c_{2nes} = \frac{C_{nes}}{\left(\frac{m}{3}+M_{nes}\right)\omega_e} \qquad k_{1nes} = \frac{K_{nes}(l\theta_0)^{n-1}}{M_{nes}\omega_e^2} \qquad k_{2nes} = \frac{K_{nes}(l\theta_0)^{n-1}}{\left(\frac{m}{3}+M_{nes}\right)\omega_e^2}$$

The physical parameters used are the following: $C_0 = 0.11$ F, $a_3 = 158\,\text{VC}^{-3}$, $Q_0 = 0.24$ C, $R = 0.97\ \Omega$, $L = 1.15$ H, $B = 0.02$ T, $N = 685$, $\theta_0 = \pi$ rad, $l = 0.465$ m, $g = 9.81$ m/s^2, $m = 1$ kg, $M_{nes} = 0.1$ kg, $\beta = 0.49$ Ns/m, $\Omega = 5.6$ rad/s, $\sigma = 0.5$, $K_{nes} = 1.5$ N/m, $C_{nes} = 0.3$ Ns/m.

This gives the following values for non-dimensional constants: $\omega = 2$, $\omega_2 = 1$, $\mu_1 = 0.30$, $\mu_2 = 0.1$, $\alpha = 1$, $\gamma_1 = 1.5$, $\gamma_2 = 0.1$, $c_{1nes} = 1$, $c_{2nes} = 5$, $k_{1nes} = 2$, $k_{2nes} = 8$.

2.4. Bifurcation structures and basin of chaoticity

The aim of this subsection is to find how chaos arises in our electromechanical model as the parameters of the system evolve. For this purpose, we numerically solve equations of motion (2.11) and plot the resulting bifurcation diagrams, Lyapunov exponents, phase planes and Poincare maps as E, ω, ω_2, α, μ_1, μ_2, γ_1, γ_2, c_{1nes}, c_{2nes}, k_{1nes}, k_{2nes} varies. Figures 2 and 3 show the non-dimensional amplitude diagram for the pendulum arm as the other non-dimensional
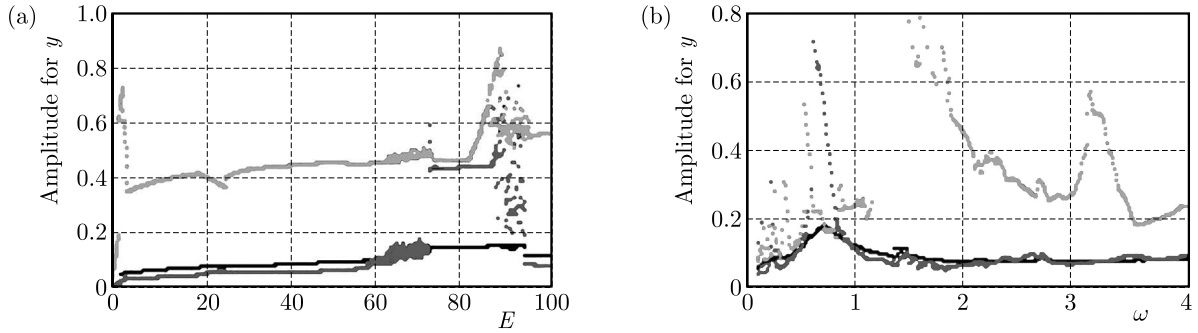
Fig. 2. Amplitude of the pendulum arm versus (a) excitation amplitude E, (b) excitation frequency ω; bleu lines $n = 1$, black lines $n = 3$, grey lines without NES
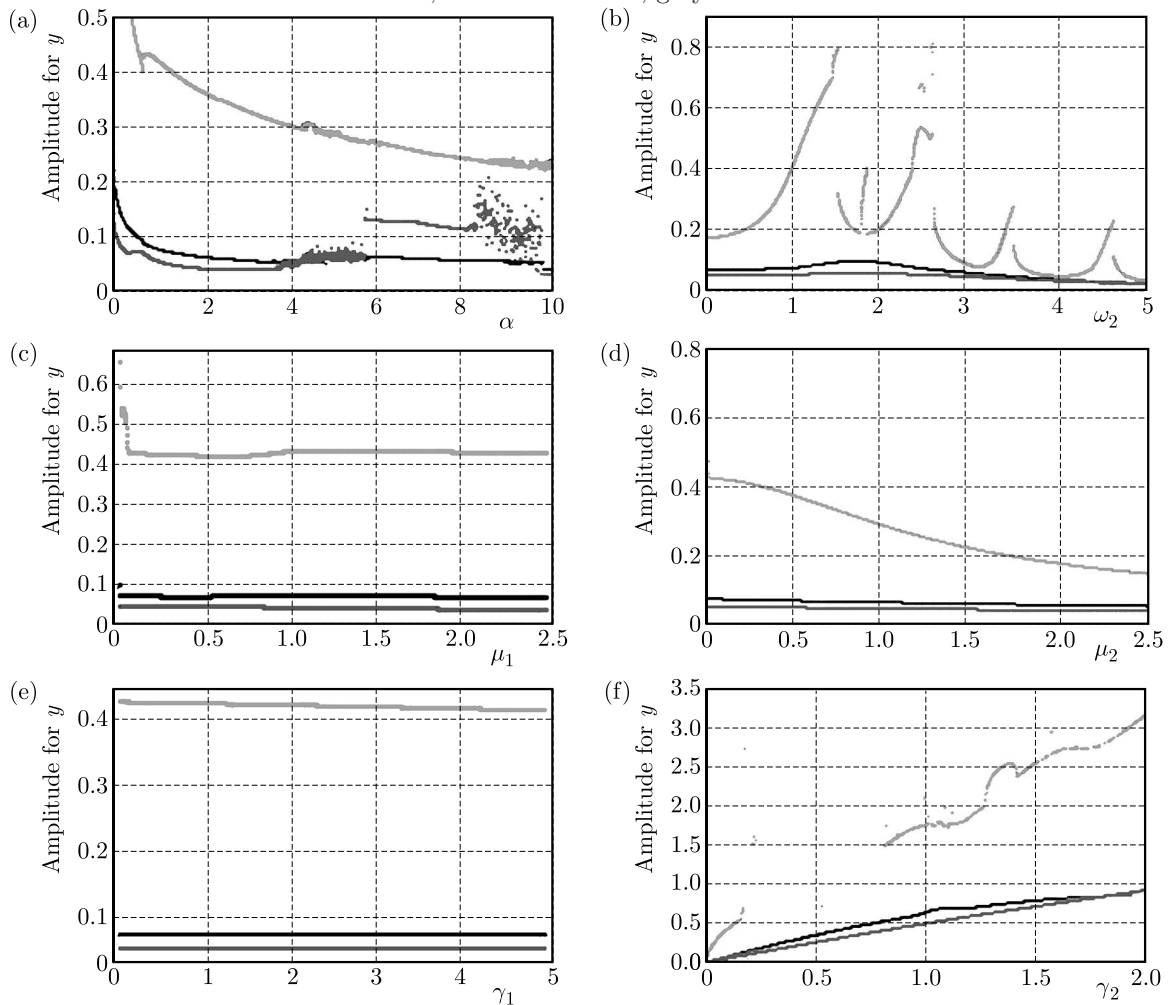
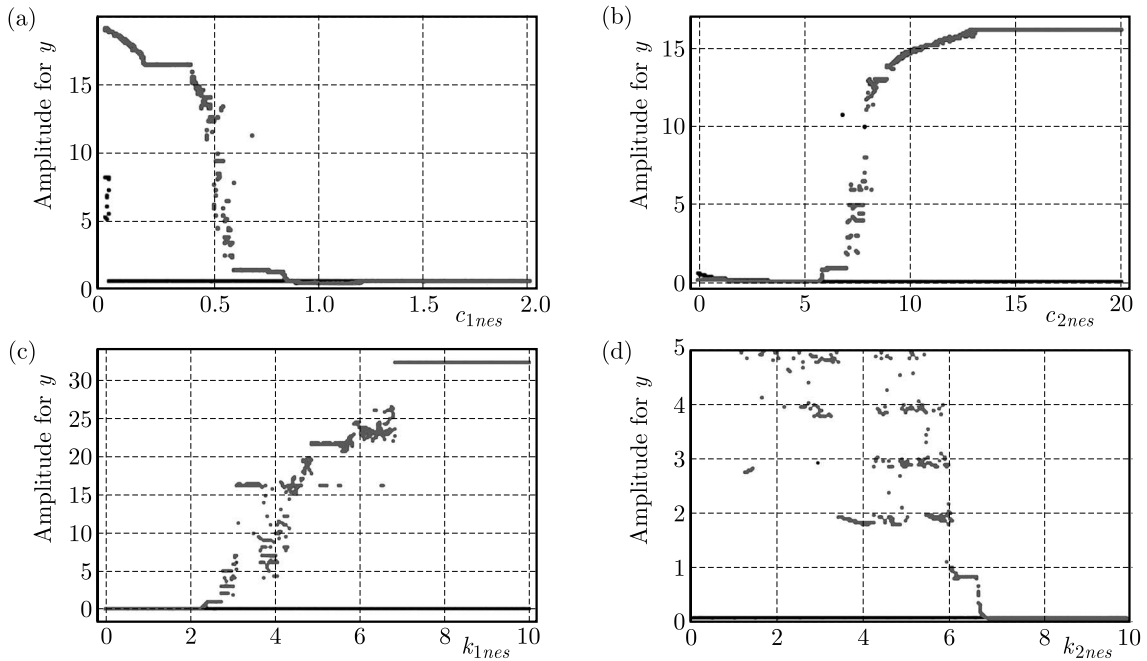Fig. 3. Amplitude of the pendulum arm versus (a) function of α, (b) function of ω_2, (c) function of μ_1, (d) function of μ_2, (e) function of γ_1, (f) function of γ_2; bleu lines $n = 1$, black lines $n = 3$, grey lines without NES

parameters (E, ω, ω_2, α, μ_1, μ_2, γ_1, γ_2) vary. The dark grey lines are shown for $n = 1$, the black lines for $n = 3$ and the grey ones for without NES. The investigation of these figures shows that the pendulum arm with NES and $n = 3$ diminishes the chaotic effect and amplitude.

Figure 4 shows the non-dimensional amplitude diagram for the pandulum arm as the other non-dimensional parameters (c_{1nes}, c_{2nes}, k_{1nes}, k_{2nes}) vary. The dark grey lines are for $n = 1$, the black lines for $n = 3$. It is clear that for $n = 3$ the chaotic effect and amplitude are diminished.

Fig. 4. Amplitude of the pendulum arm versus (a) function of c_{1nes}, (b) function of c_{2nes}, (c) function of k_{1nes}, (d) function of k_{2nes}; dark grey lines $n = 1$, black lines $n = 3$

Table 1 shows the stability condition as a function of E, ω, ω_2, α, γ_2, k_{1nes}, k_{2nes}, c_{1nes}, c_{2nes}. It has been constructed with Figs. 5-8 and Figs. 10-14. According to this Table, the pendulum arm with NES and $n = 3$ diminishes the chaotic effect and amplitude. Figure 9 shows that only for $\mu 1 < 0.01$ the system exhibits chaotic effect without NES.
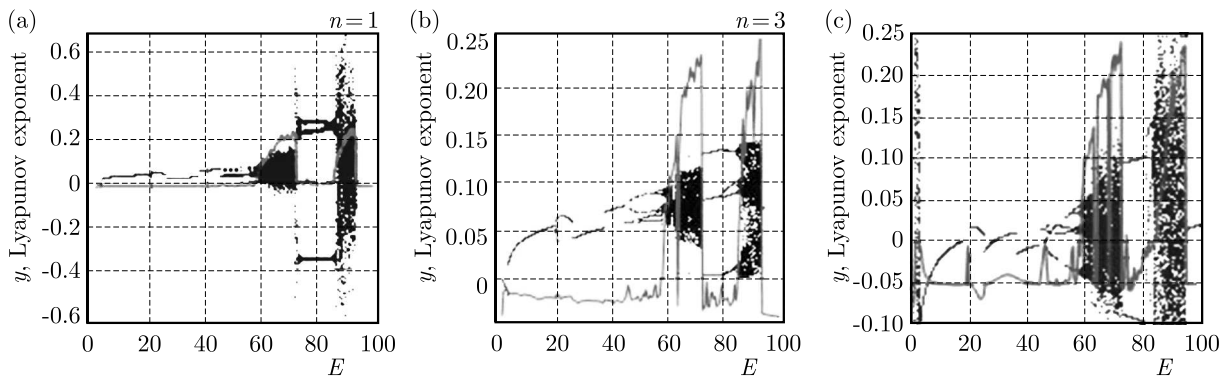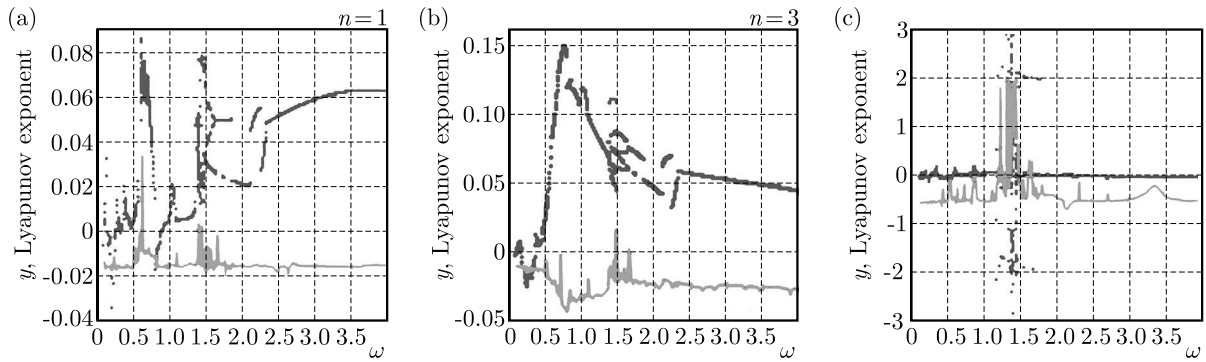

Fig. 5. Bifurcation diagrams and Lyapunov exponents of the pendulum arm as functions of E in the y direction, (a) NES, $n = 1$, (b) NES $n = 3$, (c) without NES. The other parameters are $E = 30$, $\omega = 2$, $\mu_1 = 0.3$, $\mu_2 = 0.1$, $\theta_0 = \pi$, $\gamma_1 = 1.5$, $\gamma_2 = 0.1$, $c_{1nes} = 1$, $c_{2nes} = 5$, $k_{1nes} = 2$, $k_{2nes} = 8$; dark grey line – bifurcation diagram, grey line – Lyapunov exponent

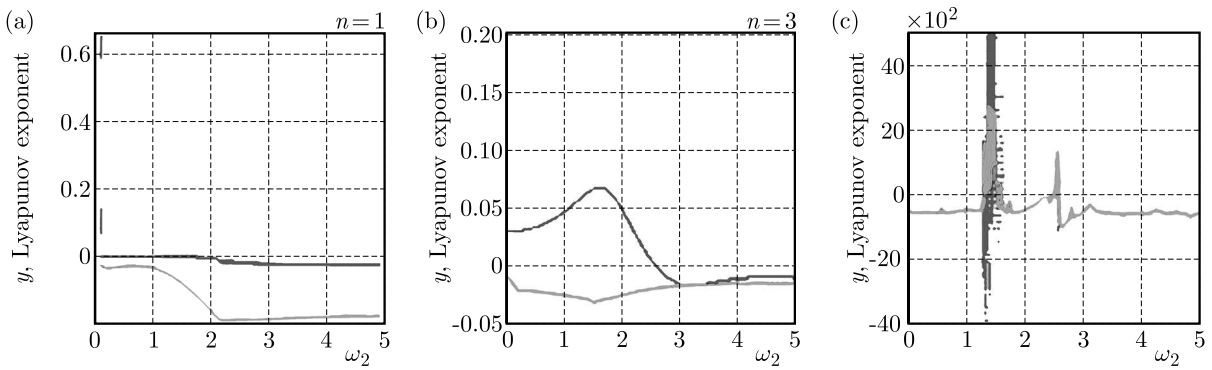Fig. 6. Bifurcation diagrams and Lyapunov exponents of the pendulum arm as functions of ω in the y direction, (a) NES, $n = 1$, (b) NES $n = 3$, (c) without NES. The other parameters are $E = 30$, $\omega_2 = 1$, $\mu_1 = 0.3$, $\mu_2 = 0.1$, $\theta_0 = \pi$, $\gamma_1 = 1.5$, $\gamma_2 = 0.1$, $c_{1nes} = 1$, $c_{2nes} = 5$, $k_{1nes} = 2$, $k_{2nes} = 8$; dark grey line – bifurcation diagram, grey line – Lyapunov exponent
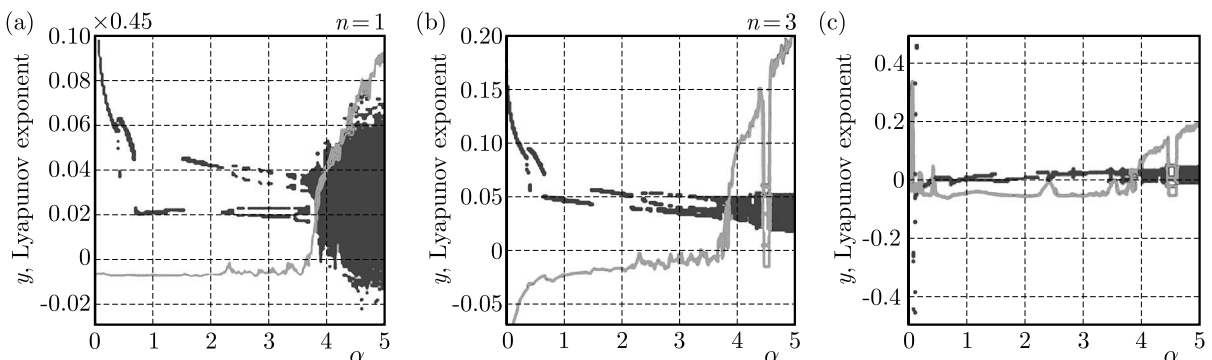

Fig. 7. Bifurcation diagrams and Lyapunov exponents of the pendulum arm as functions of ω_2 in the y direction, (a) NES, $n = 1$, (b) NES $n = 3$, (c) without NES. The other parameters are $E = 30$, $\omega = 2$, $\mu_1 = 0.3$, $\mu_2 = 0.1$, $\theta_0 = \pi$, $\gamma_1 = 1.5$, $\gamma_2 = 0.1$, $c_{1nes} = 1$, $c_{2nes} = 5$, $k_{1nes} = 2$, $k_{2nes} = 8$; dark grey line – bifurcation diagram, grey line – Lyapunov exponent
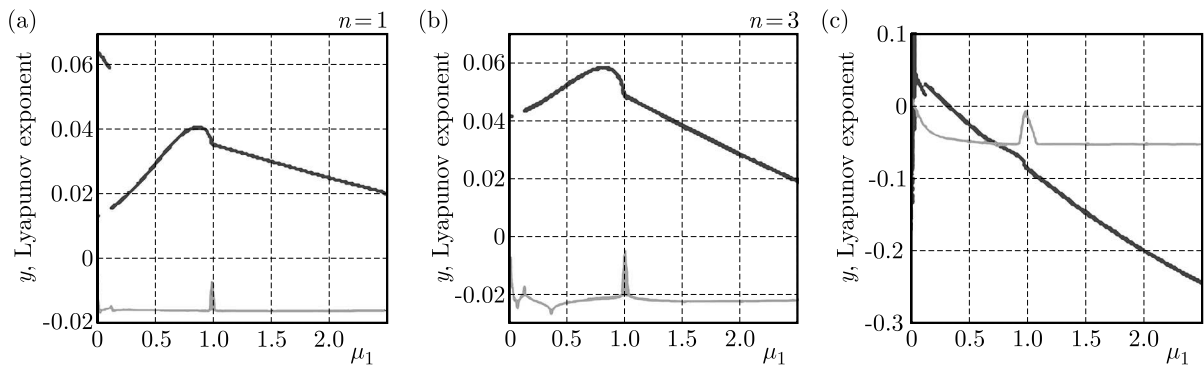

Fig. 8. Bifurcation diagrams and Lyapunov exponents of the pendulum arm as functions of α in the y direction, (a) NES, $n = 1$, (b) NES $n = 3$, (c) without NES. The other parameters are $E = 30$, $\omega = 2$, $\mu_1 = 0.3$, $\mu_2 = 0.1$, $\theta_0 = \pi$, $\gamma_1 = 1.5$, $\gamma_2 = 0.1$, $c_{1nes} = 1$, $c_{2nes} = 5$, $k_{1nes} = 2$, $k_{2nes} = 8$; dark grey line – bifurcation diagram, grey line – Lyapunov exponent
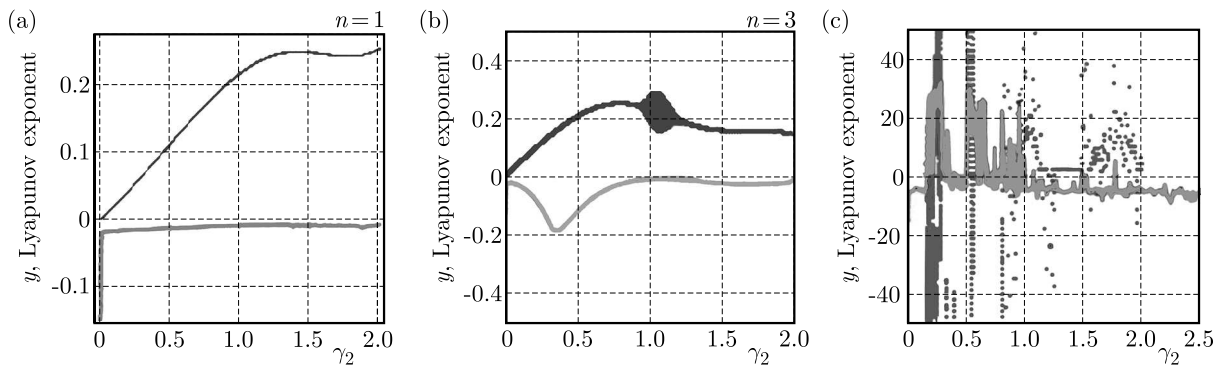
Fig. 9. Bifurcation diagrams and Lyapunov exponents of the pendulum arm as functions of μ_1 in the y direction, (a) NES, $n = 1$, (b) NES $n = 3$, (c) without NES. The other parameters are $E = 30$, $\omega = 2$, $\alpha = 1$, $\mu_2 = 0.1$, $\theta_0 = \pi$, $\gamma_1 = 1.5$, $\gamma_2 = 0.1$, $c_{1nes} = 1$, $c_{2nes} = 5$, $k_{1nes} = 2$, $k_{2nes} = 8$; dark grey line – bifurcation diagram, grey line – Lyapunov exponent

Fig. 10. Bifurcation diagrams and Lyapunov exponents of the pendulum arm as functions of γ_2 in the y direction, (a) NES, $n = 1$, (b) NES $n = 3$, (c) without NES. The other parameters are $E = 30$, $\omega = 2$, $\mu_1 = 0.3$, $\mu_2 = 0.1$, $\theta_0 = \pi$, $\alpha = 1$, $\gamma_1 = 1.5$, $c_{1nes} = 1$, $c_{2nes} = 5$, $k_{1nes} = 2$, $k_{2nes} = 8$; dark grey line – bifurcation diagram, grey line – Lyapunov exponent
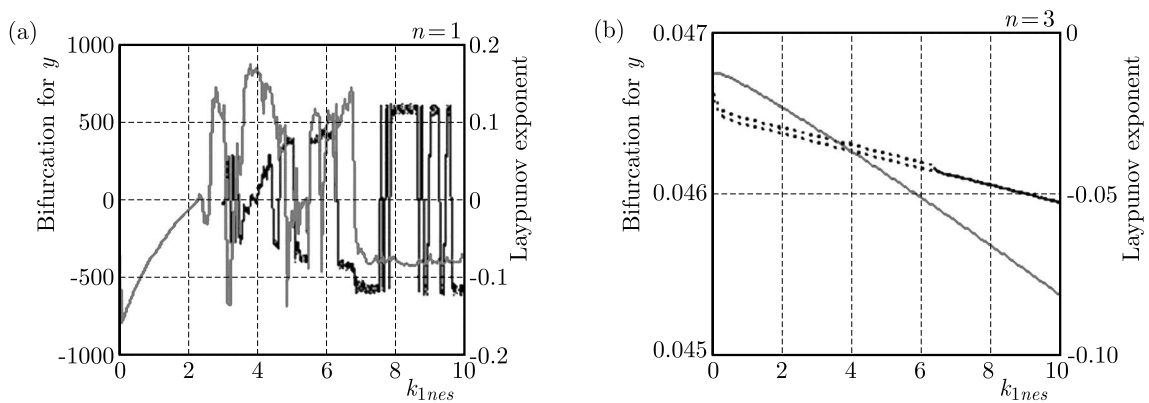

Fig. 11. Bifurcation diagrams and Lyapunov exponents of the pendulum arm as functions of k_{1nes} with NES, (a) $n = 1$, (b) $n = 3$. The other parameters are $E = 30$, $\omega = 2$, $\mu_1 = 0.3$, $\mu_2 = 0.1$, $\theta_0 = \pi$, $\alpha = 1$, $\gamma_2 = 0.1$, $c_{1nes} = 1$, $c_{2nes} = 5$, $k_{2nes} = 8$; dark grey line – bifurcation diagram, grey line – Lyapunov exponent
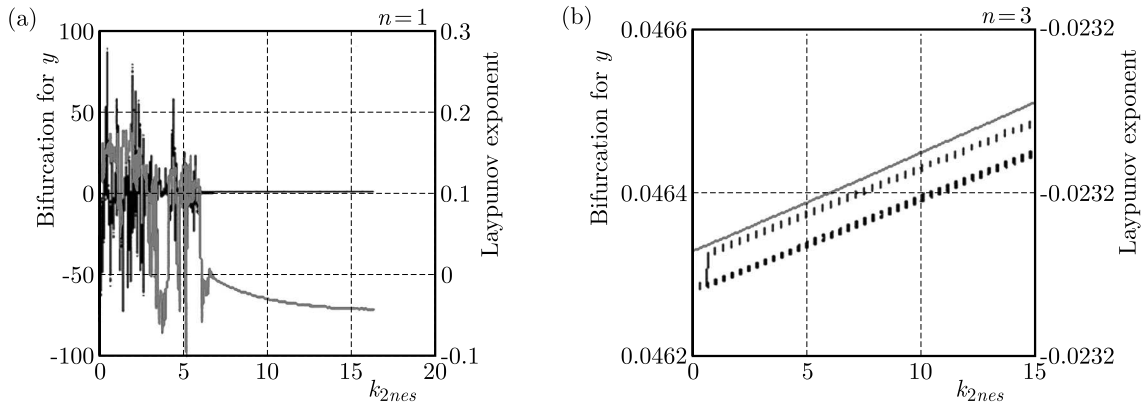
Fig. 12. Bifurcation diagrams and Lyapunov exponents of the pendulum arm as functions of k_{2nes} with NES, (a) $n = 1$, (b) $n = 3$. . The other parameters are $E = 30$, $\omega = 2$, $\mu_1 = 0.3$, $\mu_2 = 0.1$, $\theta_0 = \pi$, $\alpha = 1$, $\gamma_2 = 0.1$, $c_{1nes} = 1$, $c_{2nes} = 5$, $k_{1nes} = 2$; dark grey line – bifurcation diagram, grey line – Lyapunov exponent
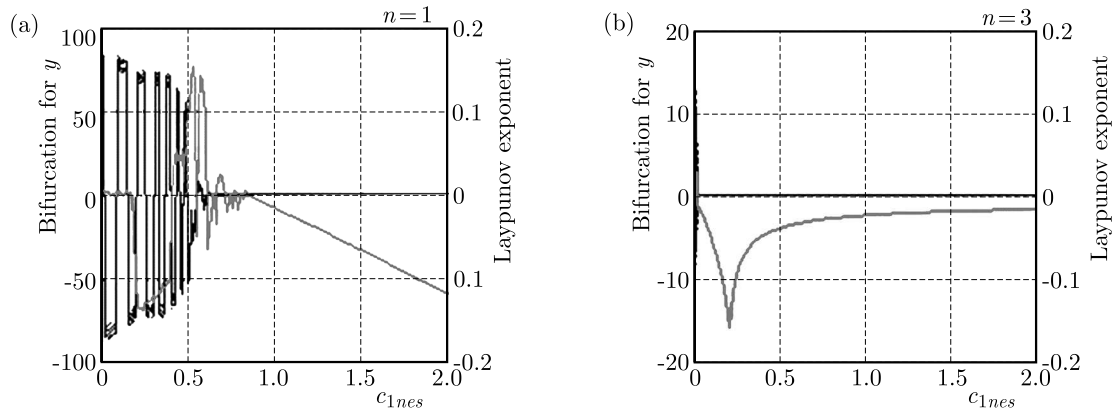

Fig. 13. Bifurcation diagrams and Lyapunov exponents of the pendulum arm as functions of c_{1nes} with NES, (a) $n = 1$, (b) $n = 3$. The other parameters are $E = 30$, $\omega = 2$, $\mu_1 = 0.3$, $\mu_2 = 0.1$, $\theta_0 = \pi$, $\alpha = 1$, $\gamma_2 = 0.1$, $c_{1nes} = 1$, $c_{2nes} = 5$, $k_{1nes} = 2$, $k_{2nes} = 8$; dark grey line – bifurcation diagram, grey line – Lyapunov exponent
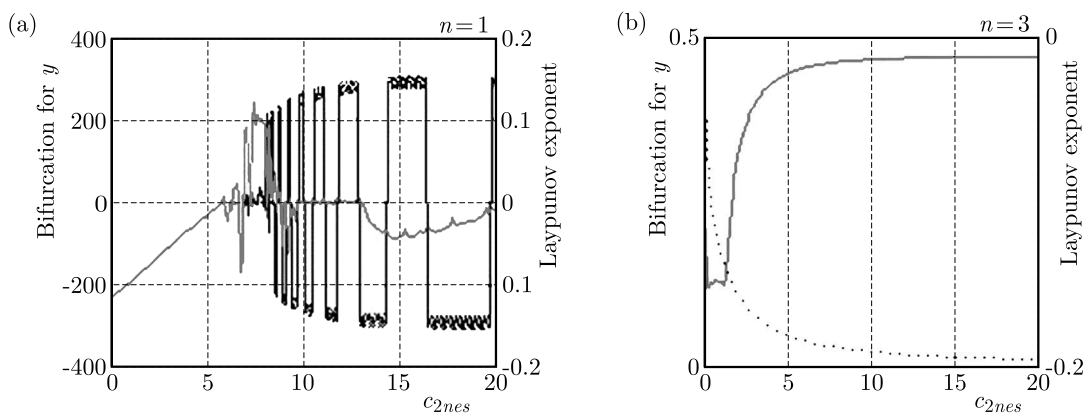

Fig. 14. Bifurcation diagrams and Lyapunov exponents of the pendulum arm as functions of c_{2nes} with NES, (a) $n = 1$, (b) $n = 3$. The other parameters are $E = 30$, $\omega = 2$, $\mu_1 = 0.3$, $\mu_2 = 0.1$, $\theta_0 = \pi$, $\alpha = 1$, $\gamma_2 = 0.1$, $c_{1nes} = 1$, $k_{1nes} = 2$, $k_{2nes} = 8$; dark grey line – bifurcation diagram, grey line – Lyapunov exponent

Table 1. Stability conditions as a function of E, ω, ω_2, α, γ_2, k_{1nes}, k_{2nes}, c_{1nes}, c_{2nes}

	Periodic	Quasi periodic	Chaotic
Fig. 5a, $n=1$, various E	$E < 45$, $E > 93$	$45 < E < 57$, $73 < E < 87$	$57 < E < 73$, $87 < E < 93$
Fig. 5b, $n=3$, various E	$E < 20$, $93 < E$, $28 < E < 45$	$20 < E < 28$, $45 < E < 58$, $72 < E < 86$	$58 < E < 72$, $86 < E < 93$
Fig. 5c, without NES, various E	$5 < E < 20$, $E > 95$	$E = 32$, $48 < E < 60$	$E < 5$, $60 < E < 73$, $85 < E < 95$
Fig. 6a, $n=1$, various ω	$\omega < 0.7$, $\omega > 2.3$	$1.5 < \omega < 1.8$, $2.1 < \omega < 2.3$	$0.7 < \omega < 0.8$, $1.3 < \omega < 1.45$
Fig. 6b, $n=3$, various ω	$\omega < 1.45$, $\omega > 2.3$	$1.5 < \omega < 1.7$	$1.45 < \omega < 1.5$, $\omega = 1.7$
Fig. 6c, without NES, various ω	$\omega < 0.4$, $\omega > 2.3$	$0.5 < \omega < 0.6$, $0.8 < \omega < 0.9$	$1.2 < \omega < 1.5$, $1.6 < \omega < 1.7$
Fig. 7a, $n=1$, various ω_2	$0 > \omega_2 < 5$		
Fig. 7b, $n=3$, various ω_2	$0 > \omega_2 < 5$		
Fig. 7c, without NES, various ω_2	$\omega_2 < 1.3$, $\omega_2 > 2.55$, $1.6 < \omega_2 < 2.5$		$1.3 < \omega_2 < 1.6$, $2.5 < \omega_2 < 2.55$
Fig. 8a, $n=1$, various α	$\alpha < 2.3$	$2.3 < \alpha < 3.7$	$\alpha > 3.7$
Fig. 8b, $n=3$, various α	$\alpha < 2.2$	$2.3 < \alpha < 3.7$, $4.4 < \alpha < 4.6$	$3.7 < \alpha < 4.4$, $\alpha > 4.6$
Fig. 8c, without NES, various α	$0.2 < \alpha < 0.4$, $0.5 < \alpha < 1$, $1.4 < \alpha < 2.2$	$1.2 < \alpha < 1.4$, $2.2 < \alpha < 3.4$, $4.4 < \alpha < 4.6$	$0 < \alpha < 0.2$, $0.4 < \alpha < 0.5$, $3.4 < \alpha < 3.6$, $3.8 < \alpha < 4.4$, $4.6 < \alpha < 5$
Fig. 10a, $n=1$, various γ_2	$0 < \gamma_2 < 2$		
Fig. 10b, $n=3$, various γ_2	$0 < \gamma_2 < 0.8$, $1.38 < \gamma_2 < 2$		$0.8 < \gamma_2 < 1.3$
Fig. 10c, without NES, various γ_2	$0 < \gamma_2 < 0.15$, $1.35 < \gamma_2 < 1.4$	$1.9 < \gamma_2 < 2.5$	$0.15 < \gamma_2 < 1.1$, $1.8 < \gamma_2 < 1.9$
Fig. 11a, $n=1$, various k_{1nes}	$0 < k_{1nes} < 2.1$	$3 < k_{1nes} < 3.2$, $4.8 < k_{1nes} < 5$, $6.4 < k_{1nes} < 10$	$2.1 < k_{1nes} < 3$, $3.1 < k_{1nes} < 5$, $5 < k_{1nes} < 6.4$
Fig. 11b, $n=3$, various k_{1nes}	$6.4 < k_{1nes} < 10$	$0 < k_{1nes} < 6.4$	
Fig. 12a, $n=1$, various k_{2nes}	$7 < k_{2nes} < 15$		$0 < k_{2nes} < 7$
Fig. 12b, $n=3$, various k_{2nes}		$0 < k_{2nes} < 15$	

Fig. 13a, $n = 1$, various c_{1nes}	$0.2 < c_{1nes} < 0.4$, $0.7 < c_{1nes} < 2$	$0 < c_{1nes} < 0.2$	$0.4 < c_{1nes} < 0.7$
Fig. 13b, $n = 3$, various c_{1nes}	$0 < c_{1nes} < 2$		
Fig. 14a, $n = 1$, various c_{2nes}	$0 < c_{2nes} < 2$		$2 < c_{2nes} < 20$
Fig. 14b, $n = 3$, various c_{2nes}	$0 < c_{2nes} < 2$		$2 < c_{2nes} < 20$

3. Conclusion

We have studied the effect of the NES on a electro-mechanical device with a pendulum.

The system exhibits complex dynamical behavior such as multi-periodic, quasi-periodic and chaotic responses, and these are strongly dependent on non-dimensional control parameters E, ω and a nonlinearity coefficient α for RLC circuit, and NES parameters c_{1nes}, c_{2nes}, k_{1nes}, k_{2nes}. Moreover, the system without NES exhibits a chaotic response depending on γ_2. The NES parameters (c_{1nes}, c_{2nes}, k_{1nes}, k_{2nes}) for $n = 1$ lead to chaotic responses, but for $n = 3$, they induce periodic and quasi-periodic responses. It is shown that the NES is capable of absorbing energy from the system and decreases the amplitude as well as diminishes the chaotic effect.

References

1. DANTAS M.J.H., BALTHAZAR J.M., 2008, On energy transfer between linear and non-linear oscillator, *Journal of Sound and Vibration*, **315**, 4/5, 1047-1070

2. FELIX J.L.P., BALTHAZAR J.M., 2009, Comments on a nonlinear and a non-ideal electromechanical damping vibration absorber, sommerfeld effect and energy transfer, *Nonlinear Dynamics*, **55**, 1, 1-11

3. FELIX J.L.P., BALTHAZAR J.M., DANTAS M.J.H., 2009, On energy pumping, synchronization and beat phenomenon in a non-ideal structure coupled to an essentially nonlinear oscillator, *Nonlinear Dynamics*, **56**, 1, 1-11

4. JIANG X., MCFARLAND D.M., BERGMAN L.A., VAKAKIS A.F., 2003, Steady state passive non-linear energy pumping in coupled oscillators: theoretical and experimental results, *Nonlinear Dynamics*, **33**, 87-102

5. MALATKAR P., NAYFEH A.H., 2007, Steady-state dynamics of a linear structure weakly coupled to an essentially nonlinear oscillator, *Nonlinear Dynamics*, **47**, 167-179

6. MOGO J.B., WOAFO P., 2007, Dynamics of a nonlinear electromechanical device with a pendulum arm, *Journal of Computational and Nonlinear Dynamics*, **2**, 4, 374-378, DOI: 10.1115/1.2756080

7. TUSSET A.M., BALTHAZAR J.M., FELIX J.L.P., 2013, On elimination of chaotic behavior in a non-ideal portal frame structural system, using both passive and active controls, *Journal of Vibration and Control*, **19**, 6, 803-813

8. TUSSET A.M., BUENO A.M., SADO D., BALTHAZAR J.M., COLÓN D., 2014, SDRE control and sensibility analysis of a chaotic double pendulum arm excited by a RLC circuit based nonlinear shaker, *Conference on Dynamical Systems Theory and Applications*, Łódź, Poland, 195-204

9. TUSSET A.M., PICIRILLO V., BUENO A.M., SADO D., BALTHAZAR J.M., FELIX J.L.P., 2015, Chaos control and sensitivity analysis of a double pendulum arm excited by an RLC circuit based nonlinear shaker, *Journal of Vibration and Control*, 1077546314564782

10. VAKAKIS A.F., 2001, Inducing passive nonlinear energy sinks in linear vibrating systems, *Journal of Vibration and Acoustics*, **123**, 3, 324-332

11. VAKAKIS F., GENDELMAN O., 2001, Energy pumping in nonlinear mechanical oscillators. II: Resonance capture, *Journal of Applied Mechanics*, **68**, 1, 42-48

12. VAKAKIS A.F., GENDELMAN O.V., BERGMAN L.A., MCFARLAND D.M., KERSCHEN G., LEE Y.S., 2008, *Nonlinear Targeted Energy Transfer in Mechanical and Structural Systems (Solid Mechanics and Its Applications)*, Springer